Mechanics of Advanced Composite Structures 3 (2016) 89-98

Semnan University

Mechanics of Advanced Composite Structures

journal homepage: http://MACS.journals.semnan.ac.ir

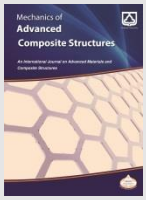

# Analytical Solution for Sound Radiation of Vibrating Circular Plates coupled with Piezo-electric Layers

**K. Khorshidi *, M. Pagoli**

*Department of Mechanical Engineering, Arak University, Arak, Iran*

**PAPER INFO**

***Paper history:***
Received: 2016-03-25
Revised: 2016-08-21
Accepted: 2016-08-28

***Keywords:***
Circular plates
Sound power
Classical plate theory
Piezoelectric layer

**ABSTRACT**

In the present study, the classical plate theory (CPT) was used to study sound radiation of forced vibrating thin circular plates coupled with piezoelectric layers using simply supported and clamped boundary conditions. The novelty of the study consists of an exact closed-form solution that was developed without any use of approximation. Piezoelectric, electrical potential loaded in the transverse direction satisfied the electric boundary conditions (open circuit) and Maxwell's electricity equation. It was assumed that no fluid loading occurred on the plate structure. The sound pressure and the sound power of the radiator were analytically obtained in a far field by using the Rayleigh integral. The proposed analytical method was validated using available data from the literature. Additionally, a few 2-D plots of the directivity pattern were illustrated for thin circular plates coupled with piezoelectric layers. Finally, the effect of boundary conditions, piezo-electric thickness, and the piezoelectric layer on the acoustical parameters were examined and discussed in details.



## 1. Introduction

Thin plates are important structural elements that are widely used in engineering applications. In particular, circular plates are employed in a wide range of engineering applications, such as aerospace structures, vehicles, ship and submarine bodies, airplane bodies and wings, and missiles.

According to classical plate theory (CPT), Wang et al. [1] analyzed the free vibration of piezoelectric coupled circular plates with clamped and simply supported boundary conditions. Their proposed model provided a good structure from which to obtain the distribution of the electric potential in piezoelectric layers. An analytical model for vibration of circular plates with piezoelectric layers was also proposed by Hagood and McFarland [2]. They assumed that the potential distribution of the circular plate in the radial direction was uniform. Heyliger and Ramirez [3] obtained free vibration characteristics of a piezoelectric circular plate, using a discrete layer employing the harmonic equations of motion. Due to the development of smart structures, elastic plates with piezoelectric elements have been studied by several researchers. In those studies, the piezoelectric layers were used as actuators and sensors to effectively control noise and vibration of these flexible structures. Therefore, the modeling and analysis of plates using piezoelectric layers are important. Hosseini-Hashemi et al. [4] and Khorshidi et al. [5] analyzed the vibration of piezoelectric, coupled, thick circular/annular functionally graded plates (FGPs) subjected to different combinations of soft simply supported, hard simply supported, and clamped boundary conditions, on the basis of Mindlin's first-order shear deformation theory (FSDT). Those studies comprehensively investigated the coupling effects between in-plane and out-of-plane displacements and boundary conditions.

Unwanted vibrations in each of these structures can result in their destruction. In addition, vibration of the plates, especially thin plates, can often be a source of noise. Excessive noise can have a serious effect on the mechanical and electrical systems by producing vibration, stress, fatigue, and failure. This sound can be created by force or dynamic torque

*Corresponding author, Tel.: +98-86-32625720; Fax: +98-86-34173450

*E-mail address:* k-khorshidi@araku.ac.ir

that is imposed on the plate. Therefore, studying the vibrational behaviors, especially the sound radiated by vibrating plates, to optimize structural design, remains a significant endeavor, and the formulation of sound power reduction appears to be necessary.

Early research efforts to calculate the radiated sound field for a flat plate in an infinite baffle dates back to the work of Rayleigh [6]. Lomas and Hayek [7] developed the Green function solution for the steady-state vibrations of an elastically supported rectangular plate coupled to a semi-infinite acoustic medium. Cremer and Heckl [8] analyzed the sound radiation of a planar source, using a Fourier transformation approach in K-space (wave number space). Berry [9] studied the sound radiation from a rectangular plate with different boundary conditions. In his work, both free and forced vibrations were considered, and the acoustic emission in the far field and sound power were calculated using a one-dimensional (1-D) Fourier transform. Yoo [10] investigated the general characteristics of sound radiation, using a point force excited rectangular plate with different boundary edge conditions. In this study, a plate under guided boundary conditions and with the critical frequency only at high frequencies was related to radiation efficiency. This approach was similar to the results that Berry achieved for one force excitation. Rdzanek [11] used closed path integral techniques and stationary phase methods to find the active and passive acoustic powers. Exact acoustical analysis of sound radiation from the free vibration of rectangular Mindlin plates, was performed by Khorshidi [12] and Hosseini-Hashemi et al. [13]. Vibration and sound radiation of a plate-ended cylindrical shells were studied by Hongqiu [14]. Zhou et al. [15] calculated the sound pressure of a thin infinite plate in contact with a layered inhomogeneous fluid subject to single point excitation. Sound radiation by the vibrational modes of baffled, flat plates was analyzed by Frank and Paolo [16]. Zhang et al. [17] obtained sound radiation from a baffled rectangular plate, which was expressed using the plate displacement function as a 2-D Fourier cosine series and the unknown Fourier expansion coefficients were determined by using the Rayleigh–Ritz procedure. Lee and Singh [18] studied the sound radiated by a thin annular plate in a far field. Lee and Singh [19] studied moderately thick, annular plates, using Mindlin plate theory in a far field. They also worked on sound radiation of thick plates and used the results to obtain a semi-analytical method for calculating sound radiation of a broken disk rotor [20].

The analytical analysis of the sound radiation of a thin circular plate exists in the literature, but this study investigated an exact closed-form formulation for the sound radiation of thin circular plates using piezoelectric layers. The novelty of the paper is that the exact closed-form solution was developed without use of approximation. The exact closed-form solution presented in this study can be used in the solution of benchmark problems for validation of future numerical methods.

First, it is assumed that no fluid loading occurs on the plate structure. To study the forced transverse vibration of thin circular plates coupled with piezoelectric layers, the equations of motion were derived based on classical plate theory. Structural-acoustic coupling was implemented for vibrating plate models. The radiation field of a vibrating plate with a specified distribution of velocity on the surface can be computed using the Rayleigh integral approach. The acoustic pressure distribution and the sound powers of the radiator were analytically obtained in its far field. The proposed analytical method was validated using available data from the literature. Additionally, a few 2-D plots of the directivity pattern are illustrated for the thin circular plates coupled with piezoelectric layers. Finally, the effect of boundary conditions, piezoelectric thickness, and the piezoelectric layer on the acoustical parameters were examined and discussed in detail.

## 2. Free Vibrations of Thin Plates with Piezoelectric Layers

A flat, piezoelectric coupled circular plate, including one host layer in the middle and two identical piezoelectric layers bonded perfectly to the upper and lower surfaces of the host layer, with outer radius $a$, host plate thickness $2h$, and piezoelectric layer thickness $h_p$, are considered as shown in Figure 1.

Both the top and bottom surfaces of each piezoelectric layer are fully covered by electrodes, which are shortly connected. The thickness of the electrodes is assumed to be extremely small compared to the plate thickness. Thus, in the following formulation, the mechanical effects of the electrodes were neglected. Both piezoelectric layers were polarized perpendicular to the mid-plane in the positive direction of the plate's thickness.

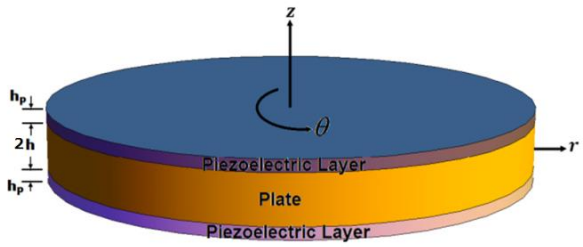


**Figure 1.** A circular plate coupled with piezoelectric layers, showing the coordinate and displacement systems.

The plate geometry and dimensions were defined in an orthogonal cylindrical coordinate system $(r,\theta,z)$, to extract mathematical formulations. The origin of the coordinate system was taken at the center of the plate in the middle plane. For convenience in the formulation, the suffixes '*p*' and '*h*' were used to denote each piezoelectric layer and the host structure, respectively.

According to the classical plate theory (CLP), the displacement field in the absence of in-plane displacements are used as follows:

$$u_z = w(r,\theta,t),$$
$$u_r = -z\,\frac{\partial w(r,\theta,t)}{\partial r}, \qquad (1a\text{-}c)$$
$$u_\theta = -z\,\frac{\partial w(r,\theta,t)}{r\partial\theta},$$

where $u_z$, $u_r$ and $u_\theta$ are the displacements in the $z$, radial, and tangential directions, respectively, and $w(r,\theta,t)$ denotes transverse displacement. The linear strain–displacement relationships were introduced to describe the deformations of the plate. The strain components $\varepsilon_{rr}$, $\varepsilon_{\theta\theta}$ and $\gamma_{r\theta}$, at an arbitrary point of the plate, are given for small deformation as [5]

$$\varepsilon_{rr} = \frac{\partial u_r}{\partial r} = -z\,\frac{\partial^2 w}{\partial r^2},$$
$$\varepsilon_{\theta\theta} = \frac{\partial u_\theta}{r\partial\theta} + \frac{u_r}{r} = -z\left(\frac{\partial^2 w}{r^2\partial\theta^2} + \frac{\partial w}{r\partial r}\right), \qquad (2a\text{-}c)$$
$$\varepsilon_{r\theta} = \frac{\partial u_r}{r\partial\theta} + \frac{\partial u_\theta}{\partial r} - \frac{u_\theta}{r} = z\left(\frac{2}{r^2}\frac{\partial w}{\partial\theta} - \frac{2}{r}\frac{\partial^2 w}{\partial r\partial\theta}\right)$$

.

Based on Hooke's law, the stress-displacement components in the host plate are expressed as follows:

$$\sigma_{rr}^{(h)} = -\frac{Ez}{1-\mu^2}\left[\frac{\partial^2 w}{\partial r^2} + \mu\left(\frac{\partial^2 w}{r^2\partial\theta^2} + \frac{\partial w}{r\partial r}\right)\right],$$
$$\sigma_{\theta\theta}^{(h)} = -\frac{Ez}{1-\mu^2}\left[\frac{\partial^2 w}{r^2\partial\theta^2} + \frac{\partial w}{r\partial r} + \mu\frac{\partial^2 w}{\partial r^2}\right], \qquad (3a\text{-}c)$$
$$\tau_{r\theta}^{(h)} = -\frac{Ez}{1+\mu}\left[\frac{\partial^2 w}{r\partial r\partial\theta} - \frac{\partial w}{r^2\partial\theta}\right],$$

where $E$ is Young's modulus, and $\mu = E/(2(1+\nu))$ is the shear modulus of the host plate. The constitutive relations in the piezoelectric layer can be written as

$$\sigma_{rr}^{(p)} = \bar{C}_{11}^E\varepsilon_{rr} + \bar{C}_{12}^E\varepsilon_{\theta\theta} - \bar{e}_{11}^E E_z,$$
$$\sigma_{\theta\theta}^{(p)} = \bar{C}_{12}^E\varepsilon_{rr} + \bar{C}_{11}^E\varepsilon_{\theta\theta} - \bar{e}_{11}^E E_z, \qquad (4a\text{-}c)$$
$$\sigma_{r\theta}^{(p)} = -z\left(\bar{C}_{11}^E - \bar{C}_{12}^E\right)\left(\frac{\partial^2 w}{r\partial r\partial\theta} - \frac{\partial w}{r^2\partial\theta}\right),$$

where $\bar{C}_{11}^E$, $\bar{C}_{12}^E$ and $\bar{e}_{11}^E$ are the reduced material constraints of the piezoelectric medium for plane stress problems given by

$$\bar{C}_{11}^E = C_{11}^E - \frac{(C_{13}^E)^2}{C_{33}^E},\ \bar{C}_{12}^E = C_{12}^E - \frac{(C_{13}^E)^2}{C_{33}^E},$$
$$\bar{e}_{11}^E = e_{11}^E - \frac{C_{13}^E e_{33}^E}{C_{33}^E} \qquad (5a\text{-}c)$$

where $C_{11}^E$, $C_{12}^E$, $C_{13}^E$, and $C_{33}^E$ are the moduli of elasticity under a constant electric field; $e_{11}^E$ and $e_{33}^E$ are the piezoelectric constants. The electric potential function is considered sinusoidal where it satisfied Maxwell's equations. Open circuit boundary conditions at the top and bottom of the piezoelectric layers are given by [4]

$$\phi = \begin{cases} \varphi(r,\theta,t)\sin\left(\pi\left(\dfrac{z-h}{h_p}\right)\right) + A_1 z + B_1 \\ h \le z \le h + h_p \\ \varphi(r,\theta,t)\sin\left(-\pi\left(\dfrac{z+h}{h_p}\right)\right) + A_2 z + B_2 \\ -(h+h_p) \le z \le -h \end{cases}, \qquad (6)$$

where $\varphi$ is the electric potential across the piezoelectric middle layer. $A_1$, $B_1$, $A_2$, and $B_2$ satisfy Maxwell's equations and open circuit boundary conditions (sensor conditions) that can be written as

$$\phi\big|_{z=\pm h} = 0,\ D_z\big|_{z=\pm(h+h_p)} = 0, \qquad (7a, b)$$

where $D_z$ is the electric displacement along the $z$ direction. The relationship between the electric field and electric displacement in the $r$, $\theta$ and $z$ directions are given by

$$E_r = -\frac{\partial\phi}{\partial r} = -\frac{\partial\varphi}{\partial r}\sin\left(\pi\left(\frac{z-h}{h_p}\right)\right) - \frac{\partial}{\partial r}(A_1 z + B_1),$$
$$E_\theta = -\frac{\partial\phi}{r\partial\theta} = -\frac{\partial\varphi}{r\partial\theta}\sin\left(\pi\left(\frac{z-h}{h_p}\right)\right) - \frac{\partial}{r\partial\theta}(A_1 z + B_1), \qquad (8a\text{-}c)$$
$$E_z = -\frac{\partial\phi}{\partial z} = -\frac{\pi}{h_p}\varphi\cos\left(\pi\left(\frac{z-h}{h_p}\right)\right) - A_1,$$

$$D_r = \bar{E}_{11}E_r\ ,\ D_\theta = \bar{E}_{11}E_\theta\ ,$$
$$D_z = \bar{e}_{31}(\varepsilon_{rr}+\varepsilon_{\theta\theta})+\bar{E}_{33}E_z\ . \tag{9a-c}$$

In Eq. (9), $\bar{E}_{11}$ and $\bar{E}_{33}$ are reductions in the dielectric constants, and they can be written as

$$\bar{E}_{11} = E_{11},\ \bar{E}_{33} = E_{33}+\left(\frac{e_{33}^E}{C_{33}^E}\right). \tag{10a, b}$$

Eqs. (10a) and (10b) satisfy both Maxwell's equations and open circuit boundary conditions (sensor conditions), so that $A_1$ and $B_1$ are given by

$$A_1 = \frac{\pi}{h_p}\varphi(r,\theta,t)-\frac{\bar{e}_{31}}{\bar{E}_{33}}\left(h+h_p\right)\Delta w\ ,$$
$$B_1 = -hA_1. \tag{11a, b}$$

The expressions for the stress resultants $M_i$ and $q_i$ $(i = r,\theta,r\theta)$ are [5]

$$M_{ii} = \int_{-h}^{h}\sigma_{ii}^h z dz + \int_{h}^{h+h_p}\sigma_{ii}^p z dz + \int_{-(h+h_p)}^{-h}\sigma_{ii}^p z dz \quad i = r,\theta,$$
$$M_{r\theta} = \int_{-h}^{h}\sigma_{r\theta}^h z dz + \int_{h}^{h+h_p}\sigma_{r\theta}^p z dz + \int_{-(h+h_p)}^{-h}\sigma_{r\theta}^p z dz\ , \tag{12a-c}$$
$$q_i = \int_{-h}^{h}\sigma_{iz}^h dz + \int_{h}^{h+h_p}\sigma_{iz}^p dz + \int_{-(h+h_p)}^{-h}\sigma_{iz}^p dz\ ,\quad i = r,\theta.$$

Based on the strain-displacement relations and stress distribution, the resultant bending moments, twisting moments, and shear forces in terms of $\varphi$ and $w$ are obtained as follows [5]:

$$M_{rr} = -\left[\left(D_1+D_2\right)\frac{\partial^2 w}{\partial r^2}+\left(\mu D_1+\frac{\bar{C}_{21}^E}{\bar{C}_{11}^E}D_2\right)\left(\frac{\partial w}{r\partial r}+\frac{\partial^2 w}{r^2\partial\theta^2}\right)+\frac{\left(\bar{e}_{31}^E\right)^2}{\bar{E}_{33}}\left(h+h_p\right)\left(\left(h+h_p\right)^2-h^2\right)\Delta w\ -\left(\frac{\left(h+h_p\right)^2-h^2}{2h_p}\pi\bar{e}_{31}^E-\frac{2\bar{e}_{31}^E}{\pi}\right)\varphi\right],$$

$$M_{r\theta} = -\left[\left(1-\mu\right)D_1+\left(1-\frac{\bar{C}_{12}^E}{\bar{C}_{11}^E}\right)D_2\right]\times\left(\frac{\partial^2 w}{r\partial r\partial\theta}-\frac{\partial w}{r^2\partial\theta}\right),$$

$$q_r = -\left(D_1+D_2+\frac{\bar{e}_{31}^E}{\bar{E}_{33}}\left(h+h_p\right)\times\left(\left(h+h_p\right)^2-h^2\right)\right)\frac{\partial}{\partial r}\left(\Delta w\right)-\left(\frac{\left(h+h_p\right)^2-h^2}{2h_p}\pi\bar{e}_{31}^E-\frac{2\bar{e}_{31}^E}{\pi}\right)\frac{\partial\varphi}{\partial r}\Bigg], \tag{13a-e}$$

$$q_\theta = -\frac{1}{r}\left(D_1+D_2+\frac{\bar{e}_{31}^E}{\bar{E}_{33}}\left(h+h_p\right)\times\left(\left(h+h_p\right)^2-h^2\right)\right)\frac{\partial}{\partial\theta}\left(\Delta w\right)-\frac{1}{r}\left(\frac{\left(h+h_p\right)^2-h^2}{2h_p}\pi\bar{e}_{31}^E-\frac{2\bar{e}_{31}^E}{\pi}\right)\frac{\partial\varphi}{\partial\theta}\Bigg],$$

where $D_1 = 2Eh^3/(3(1-\mu^2))$ and $D_2 = \frac{2}{3}((h+hp)^3-h^3)\bar{C}_{11}^E$.

The governing differential equations, based on the Kirchhoff plate theory in terms of the stress resultants using Eqs. (13a-e), can be found as

$$D\Delta\Delta w+\left(\frac{\left(h+h_p\right)^2-h^2}{2h_p}\pi\bar{e}_{31}^E-\frac{2\bar{e}_{31}^E}{\pi}\right)\Delta\varphi+2\left(\rho_h h+\rho_p h_p\right)\frac{\partial^2 w}{\partial t^2} = 0, \tag{14}$$

Note that all of the electrical variables must satisfy Maxwell's equation, which requires that the divergence of the electric flux density vanishes at any point within the media. This condition can be satisfied approximately by enforcing the integration of the electric flux divergence across the thickness of the piezoelectric layers to be zero for any $r$ and $\theta$, so the Maxwell's equation after simplifying the result gives

$$\frac{\left(\pi^2+4\right)h_p^2\bar{E}_{11}}{4\pi^2\bar{E}_{33}}\Delta\varphi-\varphi+\frac{h_p^2\bar{e}_{31}^E}{2\pi\bar{E}_{33}}\Delta w\ -\frac{h_p^3\left(h+h_p\right)}{4\pi}\frac{\bar{e}_{31}^E\bar{E}_{11}}{\left(\bar{E}_{33}\right)^2}\Delta\Delta w\ = 0. \tag{15}$$

Considering Eqs. (14) and (15), the six-order partial differential equation and the electric potential are obtained as follows

$$\varphi(r,\theta,t)=-\left(\frac{K_1 D}{K_2 d}+\frac{K_4}{K_2}\right)\Delta\Delta w+\frac{K_3}{K_2}\Delta w-\frac{K_1}{K_2}\frac{2\left(\rho_h h+\rho_p h_p\right)}{d}\frac{\partial^2 w}{\partial t^2}, \tag{16}$$

$$P_3\Delta\Delta\Delta w-P_2\Delta\Delta w+P_1\Delta\left(\frac{\partial^2 w}{\partial t^2}\right)-P_0\frac{\partial^2 w}{\partial t^2}=0, \tag{17}$$

where

$$D=D_1+D_2+\frac{\bar{e}_{31}^{E}}{\bar{E}_{33}}\left(h+h_p\right)\left(\left(h+h_p\right)^2-h^2\right),$$

$$\Delta=\frac{\partial^2}{\partial r^2}+\frac{1}{r}\frac{\partial}{\partial r}+\frac{1}{r^2}\frac{\partial^2}{\partial\theta^2},$$

$$K_1=\frac{\left(\pi^2+4\right)h_p^2\bar{E}_{11}}{4\pi^2\bar{E}_{33}},\quad K_2=1,\quad K_3=\frac{h_p^2\bar{e}_{31}}{2\pi\bar{E}_{33}}, \tag{18a-g}$$

$$K_4=\frac{h_p^3\left(h+h_p\right)}{4\pi}\frac{\bar{e}_{31}\bar{E}_{11}}{\left(\bar{E}_{33}\right)^2},$$

$$d=\frac{\left(h+h_p\right)^2-h^2}{2h_p}\pi\bar{e}_{31}^{E}-\frac{2\bar{e}_{31}^{E}}{\pi},$$

$$P_3=\frac{K_1 D+K_4 d}{K_2},\quad P_2=D,$$

$$P_1=\frac{K_1}{K_2}2\left(\rho_h h+\rho_p h_p\right), \tag{19a-d}$$

$$P_0=2\left(\rho_h h+\rho_p h_p\right).$$

After solving Eq. (17), the transverse displacement function of circular plates has taken the following form [4]

$$w(r,\theta,t)=\hat{w}(r)e^{i(p\theta-\omega t)}, \tag{20}$$

where $\hat{w}(r)$ is the transverse displacement amplitude in $z$ direction; $\omega$ is the natural frequency of the plate, and $p$ is the wavelength in $\theta$ direction. The transverse displacement amplitude is given by

$$\hat{w}(r)=A_{1p}Z_{1p}(\alpha_1 r)+A_{2p}Z_{2p}(\alpha_2 r)+A_{3p}Z_{3p}(\alpha_3 r), \tag{21}$$

where

$$\alpha_1=\sqrt{|x_1|},\qquad \alpha_2=\sqrt{|x_2|},\qquad \alpha_3=\sqrt{|x_3|},$$

$$Z_{ip}(\alpha_i r)=\begin{cases}J_p(\alpha_i r) & x_i<0\\ I_p(\alpha_i r) & x_i>0\end{cases},\quad i=1,2,3, \tag{22a-d}$$

and

$$x_1=2u\cos\left(\frac{\Psi}{3}\right)+\frac{P_2}{3P_3},$$

$$x_2=2u\cos\left(\frac{\Psi+2\pi}{3}\right)+\frac{P_2}{3P_3},$$

$$x_1=2u\cos\left(\frac{\Psi+4\pi}{3}\right)+\frac{P_2}{3P_3},$$

$$u=\frac{1}{3P_3}\sqrt{P_2^2+3P_1P_3\omega^2},$$

$$\Psi=\cos^{-1}\left[-\frac{c}{2\sqrt{(-b/3)^3}}\right], \tag{23a-g}$$

$$b=-\frac{P_2^2}{3P_3^2}-\frac{P_1\omega^2}{P_3},$$

$$c=-\frac{2P_2^2}{27P_3^2}-\frac{P_1P_2\omega^2}{3P_3^2}+\frac{P_0\omega^2}{P_3}.$$

The clamped boundary conditions along the edges of the circular plate are as follows

$$\hat{w}=\hat{w}'=\hat{\varphi}'=0. \tag{24}$$

Natural frequencies of piezoelectric coupled circular plates can be calculated by using the boundary conditions above as

$$z=\begin{vmatrix} Z_{1p}(\alpha_1 a) & Z_{2p}(\alpha_2 a) & Z_{3p}(\alpha_3 a)\\ \alpha_1 a Z'_{1p}(\alpha_1 a) & \alpha_2 a Z'_{2p}(\alpha_2 a) & \alpha_3 a Z'_{3p}(\alpha_3 a)\\ t_1\alpha_1 a Z'_{1p}(\alpha_1 a) & t_2\alpha_2 a Z'_{2p}(\alpha_2 a) & t_3\alpha_3 a Z'_{3p}(\alpha_3 a)\end{vmatrix} \tag{25}$$

where

$$t_i=-\alpha_i{}^4\left(\frac{K_1 D}{K_2 d}+\frac{K_4}{K_2}\right)+\left(\frac{K_3}{K_2}s_i\alpha_i{}^2\right)-\left(\frac{K_1}{K_2}\frac{P_0}{d}\omega^2\right)$$

and $s_i$ is the sign of $x_i$.

## 3. Forced Vibrations of a Thin Plate with Piezoelectric Layers

The equations of motion for a thin circular plate coupled with piezoelectric layers subjected to dynamic transverse loading $F$ (generated by the piezoelectric actuator) is given by

$$P_3\Delta\Delta\Delta w-P_2\Delta\Delta w+P_1\Delta\left(\frac{\partial^2 w}{\partial t^2}\right)-P_0\frac{\partial^2 w}{\partial t^2}=F(r,\theta,t). \tag{26}$$

Using the modal superposition method

$$\left(w(r,\theta,t)=\sum_{m=0}^{\infty}\sum_{n=0}^{\infty}w_{mn}(r,\theta)T_{mn}(t)\right),$$

the forced vibration of the plate is expressed as

$$\sum_{m=0}^{\infty}\sum_{n=0}^{\infty}(P_3\Delta\Delta\Delta w_{mn}-P_2\Delta\Delta w_{mn})T_{mn}(t)+ (P_1\Delta w_{mn}-P_0 w_{mn})\ddot{T}_{mn}(t)=F(r,\theta,t) \quad (27)$$

where $w_{mn}$ is the modal shape function, and $T_{mn}(t)$ is the principal coordinate for the (*m,n*) modal of the plate. Substituting Eq. (17) into Eq. (27), the governing differential equations for forced vibration of the plate are obtained as

$$\sum_{m=0}^{\infty}\sum_{n=0}^{\infty}(-\omega_{mn}{}^2(P_1\Delta w_{mn}-P_0 w_{mn}))T_{mn}(t)+ (P_1\Delta w_{mn}-P_0 w_{mn})\ddot{T}_{mn}(t)=F(r,\theta,t) \quad (28)$$

Multiplying Eq. (28) by $w_{pq}$, and integration of the summation of this equation over the plate area gives

$$\ddot{T}_{mn}(t)+\omega_{mn}{}^2T_{mn}(t)=\frac{Q_{mn}(t)}{Y_{mn}}, \quad (29)$$

where

$$Y_{mn}=\int_0^{ro}\int_0^{2\pi}(P_1\Delta w_{mn}- P_0 w_{mn})w_{pq}\,r\,dr\,d\theta=\begin{cases}0 & m,n\neq p,q\\ \neq 0 & m,n=p,q\end{cases}, \quad (30)$$

$$Q_{mn}(t)=\int_0^{ro}\int_0^{2\pi}F(r,\theta,t)w_{mn}\,r\,dr\,d\theta. \quad (31)$$

Assuming zero initial conditions, Eq. (29) is solved as

$$T_{mn}(t)=\frac{1}{Y_{mn}\,\omega_{mn}}\int_0^t Q_{mn}(\tau)\sin\left(\omega_{mn}(t-\tau)\right)\,d\tau. \quad (32)$$

Substituting Eq. (32) into

$$w(r,\theta,t)=\sum_{m=0}^{\infty}\sum_{n=0}^{\infty}w_{mn}(r,\theta)T_{mn}(t),$$

the transverse deflection of the plate due to forced vibration will be obtained as

$$w(r,\theta,t)=\sum_{m=0}^{\infty}\sum_{n=0}^{\infty}\frac{1}{Y_{mn}\,\omega_{mn}}w_{mn}(r,\theta)\times \int_0^t Q_{mn}(\tau)\sin\left(\omega_{mn}(t-\tau)\right)\,d\tau \quad (33)$$

## 4. Acoustical Radiation Field of a Thin Plate with Piezoelectric Layers

Assuming free harmonic motion, the velocity distribution on the surface of the plate may be written as

$$\dot{w}(r,\theta,t)=\sum_{m=0}^{\infty}\sum_{n=0}^{\infty}j\,\omega_{mn}w_{mn}(r,\theta)e^{j\omega_{mn}t}, \quad (34)$$

where $t$ is the time, and $j=\sqrt{-1}$. Here we assume that the circular plate radiator in flexural vibration is mounted on a flat rigid baffle of infinite extent. The coordinates shown in Figure 2 are positioned in the mid-plane surface of the plate. The acoustic pressure at the field point $P(R,\psi,\varphi)$ can be obtained by dividing the radiating surface of the flexural plate into infinitesimal elements ($ds=rdrd\theta$), where each element acts as a simple baffled source of strength having midpoint coordinates $(r,\theta)$.

The distance between the midpoint of the infinitesimal elements ($ds$) and the observation point ($P$) may be given by

$$d=\left((R\sin\psi\cos\varphi-r\cos\theta)^2+ (R\sin\psi\sin\varphi-r\sin\theta)^2+(R\cos\psi)^2\right)^{1/2}, \quad (35)$$

where $R$ is the distance between the center of the spherical coordinates and the observation point.

The critical distance $D_c$ between the near and the far fields for a vibrating plate radiator as given by Khorshidi [12] may be approximated as

$$D_c\geq 1/\lambda_{mn}, \quad (36)$$

where $\lambda_{mn}=c_0/f_{mn}$ is the wave length and $f_{mn}=\omega_{mn}/2\pi$ is the frequency of the radiated sound that is also equal to the resonance frequency of the circular plate in the flexural vibration. Using the far field approximation, the distance $d$ in the acoustic pressure amplitude can be approximated as $R$. The effect of distance on the phase of the acoustic pressure can be approximately expressed as

$$d=R-r\cos\theta\cos\varphi\sin\psi-r\sin\theta\sin\varphi\sin\psi. \quad (37)$$

Based on the theory of a Rayleigh integral [13], the total far field acoustic pressure is

$$P=\frac{j\rho_0c_0k}{2\pi d}e^{-jkR}\cos(p\varphi)\times \int_0^r\dot{w}(r,t)2\pi j^n J_n(kr\sin(\psi))rdr, \quad (38)$$

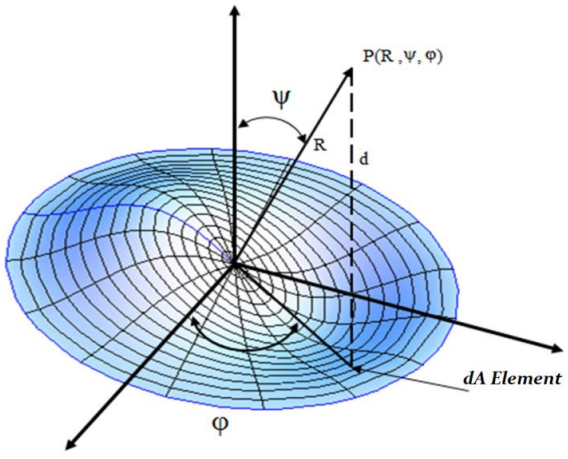


**Figure 2.** A circular plate and its field point in the spherical coordinate system.

where $k = \omega_{mn}/c_0$, $\rho_0$, and $c_0$ are the wave number, density of the medium, and speed of sound in the medium, respectively. Finally, the far field sound power of the radiator can be calculated using the following equation:

$$\Pi_{mn} = \frac{1}{2}\int_0^{2\pi}\int_0^{\pi/2} \frac{P^2}{\rho_0 c_0} R^2 \sin\psi d\psi d\varphi . \quad (39)$$

## 5. Comparison Study

In this section, to ensure the correctness of computer programs, results were compared with the results obtained by Lee and Singh [18]. Therefore, the simple annular plate without a piezoelectric layer was considered. Material and geometry characteristics of the plate appear in Table 1.

It is assumed that the boundary conditions at $r = b$ are clamped and at $r = a$ are free. Therefore, the boundary conditions are expressed as

$$M_r(a,\theta) = V_r(a,\theta) = 0,$$
$$w_r(b,\theta) = \frac{\partial w_r}{\partial r}(b,\theta) = 0. \quad (40a\text{-}d)$$

Comparison between natural frequencies obtained by the method are presented in this paper, along with the exact solution, while the results that were obtained by Lee and Singh [18] are presented in Table 2. As shown in this table, there was very good agreement between the results obtained from the current method and the Lee and Singh results. After obtaining the natural frequencies and vibration modes, we can now obtain the sound radiation of the plate. Sound powers for two modes are calculated and compared with Lee and Singh [18] in Table 3. There are two reasons for errors in the results. One reason can be attributed to the methods used to solve the problem.

**Table 1**. Material and geometry characteristics of the plate.

| | |
|---|---|
| Outer radius (mm) | 151.5 |
| Inner radius b (mm) | 82.5 |
| Radii ratio | 0.54 |
| Thickness (mm) | 31.5 |
| Thickness ratio (h/a) | 0.21 |
| Mass density (kg/m³) | 7905.9 |
| Young's modulus (GPa) | 218 |
| Poisson ratio | 0.305 |

**Table 2.** Frequencies of a thin annular plate with fixed-free boundary conditions.

| Mode sequence $(m,n)$ | $\omega_{mn}(khz)$ | | Diff. (%) |
|---|---|---|---|
| | Present | Lee and Singh [18] | |
| (0,0) | 5.478 | 5.465 | 0.24 |
| (0,1) | 5.592 | 5.580 | 0.21 |
| (0,2) | 6.097 | 6.091 | 0.098 |
| (0,3) | 7.360 | 7.360 | 0 |

In reference vibration mode shape, shapes are approximated by a polynomial, whereas in the present study an exact solution was used to obtain the vibration mode shape. Another reason is related to plate thickness and the relationship between the frequency of the classical and Mindlin plate theories. When the thickness-to-radii ratio is more than 1/20, the classical thin plate theory does not provide accurate results.

## 6. Numerical Results and Discussion

After ensuring the accuracy of the formulation in this section, numerical results were calculated, according to the developed exact solution for the sound radiation of the vibrating circular plates coupled with piezoelectric layers. Calculations have been performed for the isotropic plate (host plate), using a Poisson ratio of 0.3 and a PZT-4 piezoelectric layer by using commercial software, Mathematica (version 7). The results are presented in tabular and graphical forms for simply-supported and clamped boundary conditions, and plate and piezoelectric layer parameters. Material properties of the plate and piezoelectric layers are defined as listed in Table 4.

**Table 3.** Comparison of modal acoustic powers for two out-of-plane modes with fixed-free boundaries.

| Mode sequence (m,n) | Method | $\omega_{mn}(khz)$ | $\Pi_{mn}(pW)$ | Diff. (%) |
|---|---|---|---|---|
| (0,2) | Present | 6.097 | 84.2 | 13.1% |
| | Lee and Singh [18] | 4.85 | 73.2 | |
| (0,3) | Present | 7.360 | 86.8 | 15.1% |
| | Lee and Singh [18] | 5.71 | 73.7 | |

**Table 4**. Material properties and dimensions of the plate and piezoelectric layer [5].

| Material Property | Host plate | PZT-4 |
|---|---|---|
| $E$ (GPa) | 200 | - |
| $C_{11}^E$ (GPa) | - | 132 |
| $C_{12}^E$ (GPa) | - | 71 |
| $C_{33}^E$ (GPa) | - | 115 |
| $C_{13}^E$ (GPa) | | 73 |
| Poisson's ratio | 0.3 | - |
| Mass density (kg/m³) | 7800 | 7500 |
| $e_{31}$ (C/m$^2$) | - | -4.1 |
| $e_{33}$ (C/m$^2$) | - | 14.1 |
| $e_{15}$ (C/m$^2$) | - | 10.5 |
| $E_{11}$ ($n$ F/m) | - | 7.124 |
| $E_{33}$ ($n$ F/m) | - | 5.841 |

In Figure 3, variation of sound pressure levels of the radiated plate coupled with a piezoelectric layer versus frequency are presented for the distance between the center of the spherical coordinates and the observation point $R$ = 1.2 m, $\varphi$ = 0.6 m, and $\psi$ = 90. Acoustic frequency response function P (ω) for radius R = 1.2 m from the center of the plate and $\varphi$ = 0, $\psi$ = 90 are shown in Figure 3. The unit impulsive force was applied to the plate. As shown in Figure 3, peaks in this figure represent resonant frequencies (the undamped natural frequency of the plate is equal to the input excitation frequency). The natural frequencies of the plate were obtained using the graph acquired from the acoustic testing.

Two-dimensional directivity patterns [12, 13] of the forced vibrations of a thin circular plate with a piezoelectric layer for the first four natural frequencies are shown in Figure 4. In this figure, the relationship between sound pressure distribution and the spherical coordinate's $\psi$ is described. Results were obtained for a constant spherical coordinate's angle $\varphi$ and $\psi$ , which varies from $-\pi/2$ to $\pi/2$. As shown in Figure 4, the sound pressure distribution for the mode (m = 0, n = 0) is uniform. The directivity pattern for the mode (m = 0, n = 1,2) and (m = 1, n = 0) dipped at $\psi$ = 0, because $\psi$ = 0 is the symmetry line of the sound pressure. In a mode shape that has a line of symmetry, this line affects the sound pressure and causes a dip.

### *6.1. Effect of Boundary Conditions on Sound Power*

Acoustic sound power for the first four modes with clamped and simply supported boundary conditions are presented in Table 5. From the results displayed in Table 5, the sound powers of the vibrating plate under a clamped boundary condition were more than the sound powers of the vibrating plate under a simply supported boundary condition.

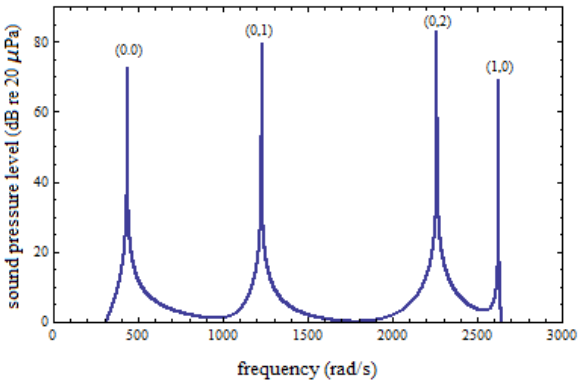


**Figure 3.** Variation of sound pressure with respect to frequanct (Acoustic frequency response function) for radius $R$ = 1.2 m, $\varphi$ = 0 , $\psi$ = 90, given unit point force excitation (simply supported BCs).

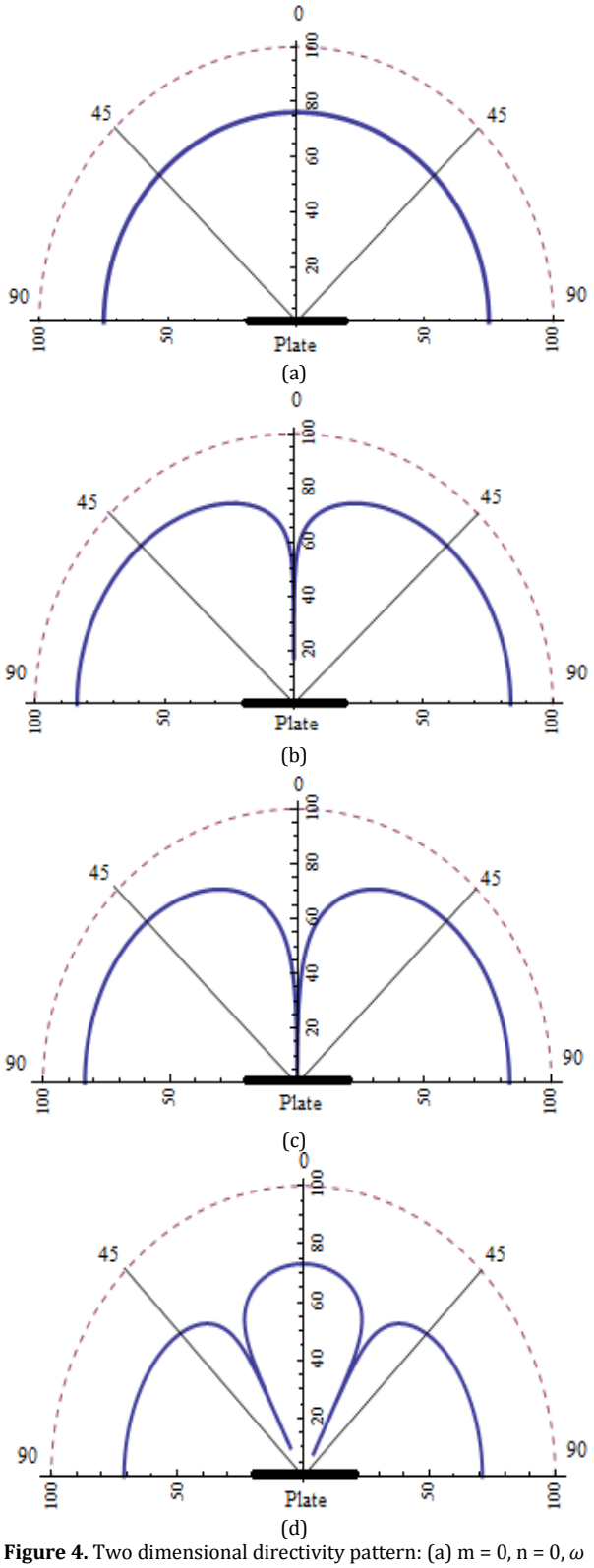


**Figure 4.** Two dimensional directivity pattern: (a) m = 0, n = 0, $\omega$ = 902.5 rad/s; (b) m = 0, n = 1, $\omega$ = 1878.2 rad/s; (c) m = 0, n = 2, $\omega$ = 3081.13 rad/s; (d) m = 1, n = 0, $\omega$ = 3513.43 rad/s.

### 6.2. Effect of Piezoelectric Thickness on Sound Power

The influence of piezoelectric thickness, *hp/2h*, on sound powers of the radiated, vibrating simply supported circular plated coupled with piezoelectric layers is examined in Table 6. The results in Table 6 are presented for the thickness ratio, *hp/2h*, which varied from 1/12 to 1/5. As the piezoelectric thickness increased, the sound power decreased. This phenomenon occurred because the transverse displacement and the transverse velocity of the plate decreased with increased piezoelectric thickness.

### 6.3. Effect of the Piezoelectric Layer on the Sound Power

In this section, to show the effects of the piezoelectric layer on the sound radiation parameters, the sound power of a radiated vibrating clamped circular plate, with and without piezoelectric layers, for the first three vibrational modes were compared and presented in Table 7. According to the results with the piezoelectric layers, natural frequencies increased about 3.7%, and sound powers increased about 9%-12% for the mode sequence (0,0), (0,1) and (0,2). Therefore, considering the inertia and stiffness of the piezoelectric layer, the vibration and sound transmission were required to obtain an accurate model for analysis.

**Table 5.** Modal acoustic powers for rgw first four out-of-plane modes with simply supported and clamped boundary conditions.

| Boundary conditions | Mode sequence | $\omega_{mn}(Hz)$ | $\Pi_{mn}(pW)$ |
|---|---|---|---|
| Simply supported | (0,0) | 69.34 | 78.88 |
| | (0,1) | 195.37 | 87.68 |
| | (0,2) | 360.08 | 93.94 |
| | (1,0) | 417.83 | 73.76 |
| Clamped | (0,0) | 143.63 | 86.6 |
| | (0,1) | 298.92 | 90.54 |
| | (0,2) | 490.37 | 94.07 |
| | (1,0) | 559.18 | 75.58 |

**Table 6.** Comparison between the sound powers $\Pi_{mn}(pW)$ of a simply supported circular plate coupled with piezoelectric layers with different piezoelectric thicknesses.

| $h_p/2h$ | Mode sequence | | | |
|---|---|---|---|---|
| | (0,0) | (0,1) | (0,2) | (1,0) |
| 1/12 | 83.35 | 87.75 | 94.05 | 73.85 |
| 1/10 | 78.88 | 87.68 | 93.94 | 73.76 |
| 1/8 | 78.83 | 87.61 | 93.82 | 73.68 |
| 1/5 | 75.78 | 87.53 | 93.71 | 73.53 |

**Table 7**. Effect of piezoelectric layers on the natural frequencies and sound powers

| Mode sequence | Parameter | Plate without Piezo | Plate with Piezo | Diff. (%) |
|---|---|---|---|---|
| (0,0) | $\omega_{mn}(rad/s)$ | 869.671 | 902.494 | 3.77 |
| | $\Pi_{mn}(pW)$ | 93.147 | 105.021 | 12.75 |
| (0,1) | $\omega_{mn}(rad/s)$ | 1810.79 | 1878.2 | 3.72 |
| | $\Pi_{mn}(pW)$ | 100.23 | 110.54 | 10.29 |
| (0,2) | $\omega_{mn}(rad/s)$ | 2969.65 | 3081.13 | 3.75 |
| | $\Pi_{mn}(pW)$ | 103.76 | 113.96 | 9.83 |

## 7. Conclusions

In this study the classical plate theory (CPT) was used to investigate the transverse sound radiation of vibrating circular plates coupled with piezoelectric layers subjected to transverse external force. The exact closed-form solution was obtained for the system with simply supported and clamped boundary conditions. The potential distribution function was earned by satisfying Maxwell's equation and boundary conditions. The frequencies, sound pressures, and sound powers of the system were presented in both tabular and graphical forms.

The significant advantages of the proposed closed-form vibro-acoustic equations consist of the following:

- These equations are capable of predicting, with high accuracy, the frequency within the validity of the CPT for an exact analytical solution.
- These equations provided a closed-form solution for sound radiation of circular plates coupled with piezoelectric layers excited by an external transverse force that can be easily solved numerically by designers and engineers.

Based on comparison with previously published results, the accuracy of the present results were validated.

## Acknowledgements

The authors gratefully acknowledge the funding by Arak University, under grant No 90/11542.

## References

[1] Wang Q Quek ST, Sun CT, Liu X. Analysis of piezoelectric coupled circular plate. *Smart Mater Struct* 2001; 10: 229-239.

[2] Hagood NW, McFarland AJ, Modeling of a piezoelectric rotary ultrasonic motor. IEEE Transactions on Ultrason, *Ferroelectrics Freq Control* 1995; 42: 210-224.

[3] HeyligerPR, Ramirez G. Free vibration of laminated piezoelectric plates and discs. *J Sound Vib* 2000; 229: 935-956.
[4] Hosseini-Hashemi Sh, Khorshidi K, Es'haghi M, Fadaee M, Karimi M. On the effects of coupling between in-plane and out-of-plane vibrating modes of smart functionally graded circular/annular plates. *Appl Math Modell* 2012; 36: 1132–1147.
[5] Khorshidi K, Rezaei E, Ghadimi AA, Pagoli M. Active vibration control of circular plates coupled with piezoelectric layers excited by plane sound wave. *Appl Math Modell* 2015; 39(3–4): 1217–1228
[6] Rayleigh L. **The Theory of Sound**, Second edition, Reprinted by Dover, New York, 1945.
[7] Lomas NS, Hayek SI. Vibration and acoustic radiation of elastically supported rectangular plates. *J Sound Vib* 1977; 2: 1–25.
[8] Cremer L, Heckl M. **Structure-Borne Sound**. Second edition, Springer-Verlag, New York, 1987.
[9] Berry A Guyader J, Nicolas, J. A general formulation for the sound radiation from rectangular, baffled plates with arbitrary boundary conditions. *J Acoust Soc Am* 1990; 88: 2792–2802.
[10] Yoo JW. Study on the general characteristics of the sound radiation of a rectangular plate with different boundary edge conditions. *J Mech Sci Technol* 2010; 24: 1111–1118.
[11] Rdzanek WP. The sound power of an individual mode of a clamped-free annular plate. *J Sound Vib* 2003; 261: 775–790.
[12] Khorshidi K. Vibro-acoustic analysis of Mindlin rectangular plates resting on an elastic foundation. *Scientia Iranica* A 2011; 18: 45–52.
[13] Hosseini-Hashemi S, Khorshidi K, Rokni Damavandi Taher H. Exact acoustical analysis of vibrating rectangular plates with two opposite edges simply supported via Mindlin plate theory. *J Sound Vib* 2009; 322: 883–900.
[14] Hongqiu L, Guoping C, Linyan X. Structural-acoustic coupling and external sound pressure of a plate-ended cylindrical shell based on analytic method, *Proc 2nd Int Conf Comput Eng Technol* 2010; 5: 51–55.
[15] Zhou L, Zheng H, Hung KC. Sound radiation from a thin infinite plate in contact with a layered inhomogeneous fluid. *Appl Acoust* 2002; 63: 1177-1192.
[16] Frank F, Paolo G. **Sound Radiation by Vibrating Structures**. Second edition, Elsevier, Academic Press, 2007; 135-241.
[17] Zhang X, Li WL. A unified approach for predicting sound radiation from baffled rectangular plates with arbitrary boundary conditions. *J Sound Vib* 2010; 329: 5307–5320.
[18] Lee M, Singh R. Analytical formulations for annular disk sound radiation using structural modes. *J Acoust Soc Am* 1994; 95: 3311–3323.
[19] Lee H, Singh R. Acoustic radiation from out-of-plane modes of an annular disk using thin and thick plate theories. *J Sound Vib* 2005; 282: 313–339.
[20] Lee H, Singh R. Determination of sound radiation from a simplified disk-brake rotor by a semi-analytical method. *Noise Control Eng J* 2004; 52: 225–239.